Low-resistance Ohmic contact of InAlN/GaN heterostructures with MOCVD-regrown n+-InGaN

Jingshu Guo, Jiejie Zhu, Siyu Liu, Jiahao Xu, Xu Zhao, Xiaohua Ma
Key Laboratory of Wide Bandgap Semiconductor Technology
School of Microelectronics, Xidian University, Xi'an 710071, China

Keywords: Gallium nitride, InAlN, regrown ohmic, MOCVD

Abstract

In this paper, the ohmic contacts of InAlN/GaN structure were realized by highly doped n^+-InGaN grown by metal-organic chemical vapor deposition (MOCVD). The square resistance of the n^+-InGaN is as low as 30Ω/□, the contact resistance between n^+-InGaN and two-dimensional electron gas(2DEG) is ~0.11Ω·mm, and the contact resistance between metal electrode and n^+-InGaN is ~0.05Ω·mm. The square resistance of the InAlN/GaN increases to 405Ω/□ after regrowth. Degradation of InAlN barrier was analyzed in detail by analysis of the lattice structure and material composition of each layer, and the way to further optimize the process of regrowth was proposed. In addition, the E-mode high electron mobility transistor (HEMT) device was fabricated and its DC characteristics were evaluated.

INTRODUCTION

GaN shows great application potential in millimeter wave and terahertz amplifiers due to its excellent material characteristics, such as high mobility, high breakdown electric field, high electron saturation rate, etc.[1-3] Deeply-scaled devices with high Al components are put forward to achieve the high frequency. But the low resistances ohmic contact of such materials with high Al components is more difficult to achieve. The larger ohmic contact resistance will lead to a significant decrease in the output power and efficiency of the device. [4-6] Several approaches have been reported to obtain excellent ohmic contact with low contact resistance and smooth surface morphology, in which regrown ohmic contact has shown great advantages in the application of high-frequency devices. Compared with traditional alloying ohmic contact, regrown ohmic can not only realize low contact resistance, and there is no metal diffusion occurs. Therefore, device with smaller size and smaller on-resistance can be achieved. Most of the reported unalloyed low-resistance ohmic are achieved by Molecular Beam Epitaxy (MBE). [7-11] However, the process has a slow film growth rate and a long material growth cycle, which is not conducive to mass production. Metal Organic Chemical Vapor deposition (MOCVD) can also achieve low-resistance ohmic contact. In addition, the process is more mature and can be used for mass production. But there are few reports about this.

In this paper, the ohmic contacts of InAlN/GaN structure was realized by MOCVD grown n^+-InGaN with the contact resistance between n^+-InGaN and 2DEG of 0.11Ω·mm. And the sheet resistance of InAlN/GaN after regrown process increases to 405Ω/□. The mechanism of the slight increase in sheet resistance after the regrowth process was investigated, which was mainly attributed to the interdiffusion of Ga and In between n^+-InGaN and InAlN layers during high-temperature MOCVD regrowth. According to the analysis, the possible direction of further improvement of the process is also pointed out.

EXPERIMENTAL PROCEDURE

The process of ohmic regrown by MOCVD is shown in Figures 1(a)-1(e). Firstly, the ohmic region was defined, and InAlN and GaN in this region were removed by dry etching to ensure contact with the 2DEG. Wet treatment had been carried out to remove surface impurities before n^+-InGaN was grown. Then, 150nm-thick n^+-InGaN with Si doping concentration of $1.5\times10^{20}cm^{-3}$ was grown by MOCVD. Next, Ti/Au electrodes were prepared over n^+-InGaN in the source/drain region by electron beam evaporation. Finally, the n^+-InGaN covering the barrier was removed. The transmission line models (TLM) used to extract contact resistance and material resistance were shown in Fig 1(f).

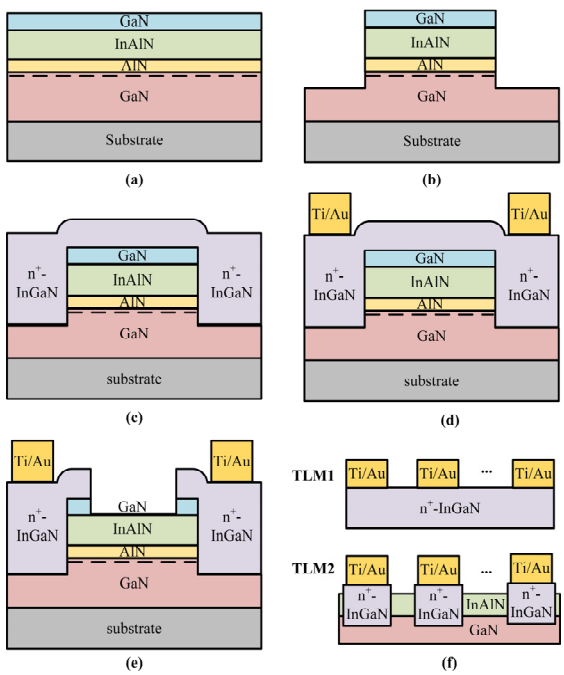

Fig. 1. (a)-(e)The regrowth process of MOCVD based on InAlN/GaN. (f) The TLM test structures.

RESULTS AND DISCUSSIONS

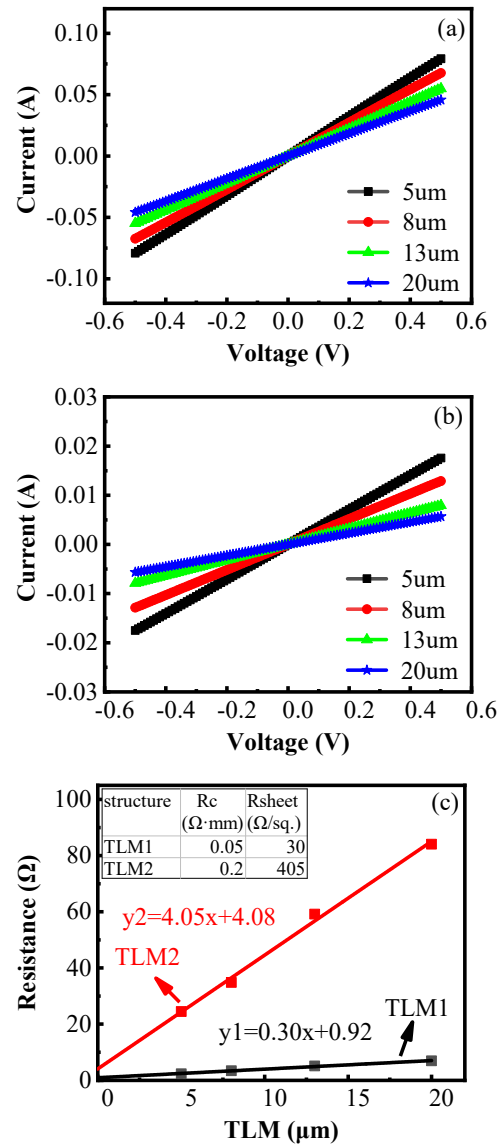

Fig. 2. *I-V* curves of TLM structures with different transmission length: (a)TLM1 and (b)TLM2. (c) shows the results of linear fitting and extraction of resistance parameters for these two TLM structures.

Current-voltage (*I-V*) curves of the two TLM structures with different transmission length were shown in Figs. 2(a) and 2(b), respectively. The linearity of the *I-V* relationship indicates good ohmic contacts. The results of linear fitting and extraction of resistance parameters for these two TLM structures were shown in Fig. 2(c). The contact resistance at the interface between metal electrode and n^+-InGaN obtained from TLM1 is 0.05 Ω·mm, the square resistance of n^+-InGaN material is 30 Ω/□. According to TLM2, the total ohmic resistance is ~0.2 Ω·mm. The calculated contact resistance between n^+-InGaN and 2DEG is ~0.11 Ω·mm, which is an obviously small contact resistance of

InAlN/GaN structure realized by MOCVD. The square resistance of the InAlN/GaN structure is 405 Ω/□, greater than that of annealed samples at the same temperature and time. That is, the InAlN barrier is affected by the MOCVD process in addition to the high temperature.

The ohmic contact profile after ohmic regrowth is shown in Fig. 3. The InAlN barrier edge is in good contact with n^+-InGaN, so the contact resistance between n^+-InGaN and 2DEG is small. It could be seen that both of the InGaN grown by MOCVD and the InAlN after the MOCVD regrowth process have high crystallinity. The MOCVD process did not result in a large number of defects in the InAlN.

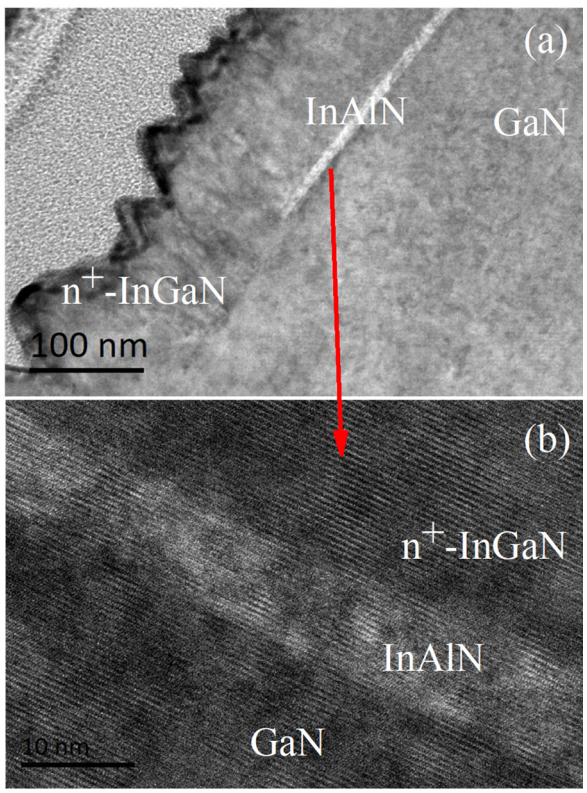

Fig. 3. (a) Cross-sectional TEM images of the ohmic structure and (b) InAlN/GaN with MOCVD regrown n^+-InGaN.

Detailed analysis on material components of InAlN after epitaxy of InGaN was conducted by Time of Flight Secondary Ion Mass Spectrometry (TOF-SIMS). Results are shown in Fig. 4. It can be seen that there was no steep step at the interface of the InAlN/GaN, which is obviously related to internal diffusion. Obviously, diffusion of Ga has a significant effect on the barrier layer and AlN spacer. These eventually lead to the gradient-component heterojunction with a shallower potential well after MOCVD regrowth. [12] The weakened quantum confinement effect on electrons results in the enhanced scattering effect and decreases the field-effect mobility of electrons. So, the sheet resistance of InAlN/GaN increase. Covering the InAlN with a diffusion impervious layer and reducing the temperature of the MOCVD regrowth process appropriately will be beneficial to further optimizing the regrown ohmic contact for InAlN/GaN HEMTs.

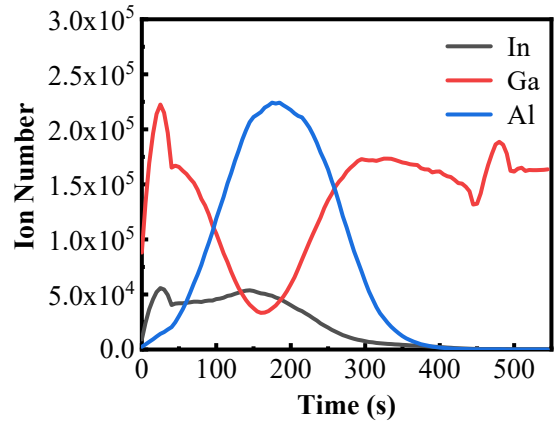

Fig. 4. TOF-SIMS analysis of InAlN/GaN after growth of n^+-InGaN.

InAlN/GaN HEMTs with MOCVD regrown n^+-InGaN were fabricated and illustrated in Fig. 5(a). The gate length (L_g) and the distance between the source and drain (L_{sd}) were 1 and 9 µm, respectively. Figures 5(a) and (b) show the transfer characteristic and output characteristic. The maximum transconductance of the E-mode HEMTs is higher than 250 mS/mm and the output saturation current is greater than 530mA/mm. The on-resistance of the device is about 4.3Ω·mm. According to the above analysis results, this value can be further reduced by covering the InAlN with a diffusion impervious layer or reducing the temperature of the MOCVD regrowth process.

CONCLUSIONS

In conclusion, low-resistance ohmic contact is formed on InAlN/GaN by MOCVD regrown n^+-InGaN. The InAlN was affected by the MOCVD process and the square resistance of InAlN/GaN heterojunction slightly increase to 405 Ω/□. The SIMS analysis showed that the Ga components significantly diffused during the MOCVD process, which results in a gradient region in the InAlN/GaN. As the potential well at heterojunction interface becomes shallower and the scattering effect becomes stronger, the decrease in carrier mobility leads to the increase in 2DEG sheet resistance. The large square resistance results in the on-resistance of the E-mode HEMT device up to 4.3 Ω·mm. Covering the InAlN with a diffusion impervious layer and reducing the temperature of the MOCVD regrowth process will be beneficial to attenuate the effect on the barrier and further optimize the performance of InAlN/GaN HEMTs.

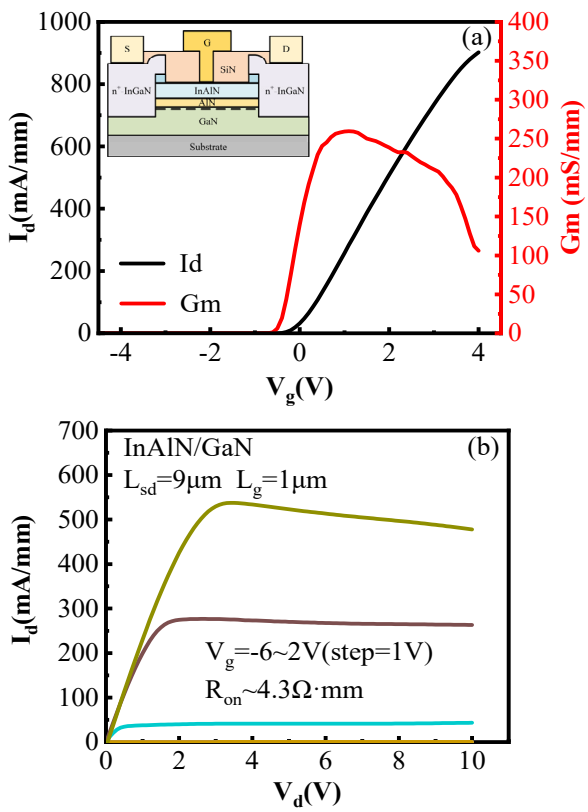

Fig. 5. (a) transfer characteristic curve and (b) the I_d–V_d characteristics of the InAlN/GaN HEMTs.

ACKNOWLEDGMENTS

This work was supported in part by the National Key R&D Program of China under Grant 2020YFB1807403, in part by the National Natural Science Foundation of China under Grant 62174125, 62131014, in part by the Fundamental Research Funds for the Central Universities under grant NO. QTZX2172, in part by the Innovation Fund of Xidian University. The MOCVD regrowth process was accomplished in collaboration with Enkris Semiconductor Inc. The TOF-SIMS analysis was achieved in collaboration with ULVAC-PHI, INC and PHI-CHINA.

REFERENCES

[1] Y. Tang, K. Shinohara, D. Regan, A. Corrion, D. Brown, J. Wong, A. Schmitz, H. Fung, S. Kim, and M. Micovic, IEEE Electron Device Lett. 36(6), 549-551 (2015).

[2] Y. K. Yadav, B. B. Upadhyay, M. Meer, Navneet Bhardwaj, S. Ganguly, and D. Sahaet, IEEE Electron Device Lett. 40(1), 67-70 (2019).

[3] X. Lu, J. Ma, H. Jiang, C. Liu, P. Xu, and K. M. Lau, IEEE Trans. Electron Devices. 62(6), 1862-1869 (2015).

[4] M. Hou, G. Xie, and K. Sheng, IEEE Electron Device Lett. 39(8), 1137-1140 (2018).

[5] L. Q. Zhang, J. S. Shi, H. F. Huang, X. Y. Liu, S. X. Zhao, P. F. Wang, and D. W. Zhang, IEEE Electron Device Lett. 36(9), 896-898 (2015).

[6] C. W. Tsou, H. C. Kang, Y. W. Lian, and S. Hsu, IEEE Trans. Electron Devices. 63(11), 4218-4225 (2016).

[7] Y. Lu, X. Ma, L.Yang, B. Hou, M. Mi, M. Zhang, J. Zheng, H. Zhang, and Y. Hao, IEEE Electron Device Lett. 39(8), 1137-1140 (2018).

[8] A. J. Tzou, D. H. Hsieh, S. H. Chen, Z. Y. Li, C. Y. Chang, and H. C. Kuo, Semicond. Sci. Technol. 31 (5), 055003 (2016)

[9] J. Guo, Y. Cao, C. Lian, T. Zimmermann, G. Li, J. Verma, X. Gao, S. Guo, P. Saunier, M. Wistey, D. Jena, and H. G. Xing, Phys. Status Solidi A 208(7), 1617–1619 (2011).

[10] D. S. Lee, X. Gao, S. Guo, D. Kopp, P. Fay, and T. Palacios, IEEE Electron Device Lett. 32(11), 1525-1527 (2011).

[11] L. Lugani, M. Malinverni, S. Tirelli, D. Marti, E. Giraud, J. F. Carlin, C. R. Bolognesi, and N. Grandjean, Appl. Phys. Lett. 105(20), 202113 (2014).

[12] J. Wang, F. Xu, X. Zhang, W. An, X. Z. Li, J. Song, W. Ge, G. Tian, J. Lu, X. Wang, N. Tang, Z. Yang, W. Li, W. Wang, P. Jin, Y. Chen, and B. Shen, Scientific Reports 4(1), 6521 (2014).